Fe Spin Reorientation across the Metamagnetic Transition in Strained FeRh Thin Films

C. Bordel, J. Juraszek, David W. Cooke, C. Baldasseroni, S. Mankovsky, J. Minár, H. Ebert, S. Moyerman, E. E. Fullerton, and F. Hellman

Phys. Rev. Lett. **109**, 117201 — Published 10 September 2012

DOI: 10.1103/PhysRevLett.109.117201

Fe spin reorientation across the metamagnetic transition in strained FeRh thin films

C. Bordel,[1,2*] J. Juraszek,[2] David W. Cooke,[1] C. Baldasseroni,[3] S. Mankovsky,[4] J. Minár,[4] H. Ebert,[4] S. Moyerman,[5]

E.E. Fullerton[5] and F. Hellman[1,6]

[1] *Department of Physics, University of California, Berkeley, Berkeley, California 94720, USA*

[2] *GPM, UMR CNRS 6634, Université de Rouen, Av. de l'Université - BP12, 76801 St Etienne du Rouvray, France*

[3]*Department of Materials Science and Engineering, University of California - Berkeley, Berkeley, California 94720, USA*

[4] *Dept. Chemie und Biochemie, Physikalische Chemie, Universität München, Butenandtstr. 5-13, 81377 München, Germany*

[5]*Center for Magnetic Recording Research, University of California, San Diego, La Jolla, California 92093*

[6] *Materials Sciences Division, Lawrence Berkeley National Laboratory, Berkeley, California 94720, USA*

ABSTRACT

A spin reorientation accompanying the temperature-induced antiferromagnetic (AFM) to ferromagnetic (FM) phase transition is reported in strained epitaxial FeRh thin films. ^{57}Fe conversion electron Mössbauer spectrometry showed that the Fe moments have different orientations in FeRh grown on thick single-crystalline MgO and in FeRh grown on ion-beam-assist-deposited (IBAD) MgO. It was also observed, in both samples, that the Fe moments switch orientations at the AFM to FM phase transition. Perpendicular anisotropy was evidenced in the AFM phase of the film grown on IBAD MgO and in the FM phase of that grown on regular MgO. Density functional theory calculations enabled this spin reorientation transition to be accurately reproduced for both FeRh films across the AFM-FM phase transition and show that these results are due to differences in strain.

* Electronic address: cbordel@berkeley.edu

PACS: 75.30.Gw, 76.80.+y, 71.15.Mb, 75.50.Bb, 75.50.-y

Equiatomic FeRh has raised a growing interest in the last decade because of the fundamental properties of its first order phase transition [1-6] as well as its potential applications in thermally-assisted magnetic recording (TAMR) [7-8]. The occurrence of a temperature- or field-induced metamagnetic transition from antiferromagnetic order (AFM) to ferromagnetic order (FM) ~350 K makes it a very interesting material for storage media applications [7].

The existence of a magnetic phase transition in equiatomic FeRh was seen by Fallot in 1938 [9], but it was only in 1961 that the low-temperature phase was identified as AFM, as reported by de Bergevin and Muldawer [10,11], and later confirmed by Kouvel and Hartelius [12] and Shirane *et al.* [13]. Note that the magnetic phase transition is accompanied by a lattice expansion of ~1% from the AFM phase to the FM phase. However, the origin of the transition is still debated. The different origins suggested in the literature range from an increase in the electronic density of states (DOS) [14,15] to spin-wave excitations [3] and instability of the Rh magnetic moment [2,6]. An increased DOS in the FM phase was experimentally seen [16] but it is insufficient to account for the large entropy change at the transition. In addition, an excess specific heat was observed in the FM phase [17], consistent with magnetic contributions to the entropy. It appears likely that the transition is caused by a combination of these phenomena. Time-resolved magneto-optical Kerr effect measurements showed that the lattice expansion occurs later than the onset of ferromagnetism in the photon-induced AFM-FM phase transition [18,19]. However, recent time-resolved X-ray circular dichroism [20] and a combination of time-resolved X-ray diffraction and magneto-optical Kerr effect experiments [21] did not confirm this result and suggest that magnetic and structural changes through the transition occur simultaneously.

In this letter, we report on the study of the AFM-FM transition in epitaxially grown FeRh films by ^{57}Fe conversion electron Mössbauer spectroscopy (CEMS). Such a microscopic technique is a very sensitive tool for the investigation of the magnetic properties of Fe-based thin films *via* nuclear hyperfine interactions [22-25]. In particular, this technique enables us to determine the direction of the magnetic moment of the Fe atoms with respect to the incident γ-radiation in both AFM and FM phases. CEMS allowed a spin-reorientation transition to be observed through the AFM-FM transition, *i.e.* the preferred direction of the Fe magnetic moments changes between the AFM and FM phases. Using density-functional theory (DFT), we show that the spin-reorientation transition is well understood as a result of an electronic structure modification under tetragonal lattice distortion, leading to a different magnetocrystalline anisotropy (MCA) for the FM and AFM states of these thin film samples.

~ 150 nm thick $Fe_{0.98}Rh_{1.02}$ films were grown epitaxially at 573 K by magnetron sputtering from an equiatomic FeRh target onto both a thick single-crystal (001) MgO substrate and an *a*-SiO_x/Si substrate coated with ion-beam-assist-deposited (001) MgO (IBAD MgO) [26]. This IBAD growth produces a biaxially-textured MgO film, whose lattice parameters are given in [26], onto which an epitaxial body-centered tetragonal FeRh film can be grown. The samples were post-annealed for 2 hours at 873 K. The composition of the films was determined via Rutherford back-scattering (RBS) measurements, and both

films were shown to be epitaxial by four-circle X-ray diffraction (XRD) which showed four in-plane (110) peaks. Temperature-controlled XRD data in the temperature range 300-500 K showed a tetragonal distortion of the films, particularly in the AFM phase of the $Fe_{0.98}Rh_{1.02}$ film grown on IBAD MgO ($Fe_{0.98}Rh_{1.02}$//IBAD MgO). The volume expansion experienced by the material at the transition temperature from the AFM to the FM phase manifests itself by an increase in the out-of-plane lattice parameter *c* because *a* and *b* are constrained by the substrate, as verified experimentally. Because films typically relax strain by nucleating defects, a higher strain is likely in thinner films. The lattice constants of the two samples in both magnetic phases are listed in Table I. The expected CsCl (B2) order was confirmed by Mössbauer spectrometry, as explained below.

^{57}Fe CEMS measurements were carried out under normal incidence with a helium-methane gas proportional counter [25], with ^{57}Co in a Rh matrix as the source. The samples were measured across the magnetic phase transition in zero magnetic field in the temperature range 293-500 K upon heating and cooling. The least-squares fit to the data was performed using the histogram method [27]. The direction of an Fe magnetic moment can be determined from the line intensity ratio (x) of the second (or fifth) and the third (or fourth) line of the magnetically-split Mössbauer sextet. The x ratio is related to β, the angle between the local magnetic hyperfine field (B_{hf}) at the ^{57}Fe nucleus and the incident γ-ray direction, by $\cos^2 \beta = (4-x)/(4+x)$. For incident γ-rays perpendicular to the sample plane, x changes from 4 to 0, for in-plane (β=90°) and out-of-plane (β=0°) spin configurations, respectively [28].

At room temperature (AFM phase), the Mössbauer spectrum for both samples displays a single magnetic six-line pattern, reflecting the high degree of chemical ordering of the films (Figs. 1(a,b)). The hyperfine parameters derived from the fit (isomer shift δ = 0.01 mm.s^{-1} and hyperfine field B_{hf} = 25 T) are close to previously reported bulk values in the AFM phase [13]. The line intensity ratio x clearly indicates that $Fe_{0.98}Rh_{1.02}$//MgO exhibits in-plane Fe magnetic moments, whereas $Fe_{0.98}Rh_{1.02}$//IBAD MgO exhibits almost out-of-plane Fe magnetic moments in the AFM phase. For the latter, the fact that the 2nd and 5th Mössbauer lines are not completely absent, as it should be for a truly perpendicular orientation of the Fe magnetic moments, is attributed to the imperfect collimation of the γ-ray beam. For $Fe_{0.98}Rh_{1.02}$//MgO heated up to 450 K (FM phase), $x \sim 2$ (Fig. 1(c)), corresponding to a broad distribution of spin orientation and indicating that for this sample, the Fe spin orientation in the FM phase no longer lies in the film plane. This will be explained on the basis of the DFT calculations. On the contrary, for $Fe_{0.98}Rh_{1.02}$//IBAD MgO measured upon cooling at 340 K (FM phase), the increase of the line intensity x up to ~ 4 on the Mössbauer spectrum indicates a spin reorientation transition from out-of-plane in the AFM phase to in-plane in the FM phase (Fig. 1(d)).

The hyperfine field plotted as a function of temperature (Figs. 2(a,b)) shows that the local magnetic moment carried by Fe is higher in the FM phase than in the AFM phase for both samples, in agreement with results obtained on bulk samples [13] and polycrystalline thin films [29]. The hysteretic behaviour of the hyperfine field as a function of temperature is seen, and the transition temperature upon heating is

found to be 390±10 K for $Fe_{0.98}Rh_{1.02}$//MgO (Fig. 2(a)) and 350±10 K for $Fe_{0.98}Rh_{1.02}$//IBAD MgO (Fig. 2(b)), in good agreement with the macroscopic magnetization data (Figs. 2(c,d)). SQUID magnetometry measurements show that the transition temperature (extrapolated in zero field) is 380±10 K for the sample grown on MgO (Fig. 2(c)) and 340±10 K for the sample grown on IBAD MgO (Fig. 2(d)), and in both cases the magnetization above the transition is ~1100 emu/cm^3 (1.1×10^6 A/m), in good agreement with previously reported values [30]. This result suggests a decrease in transition temperature under the influence of tensile strain, as observed in [30]. Although further investigation is underway, we hypothesize that the larger in-plane lattice constant generated by *c*-axis sapphire in [30] and IBAD MgO in this present work provides a closer match to the FeRh FM phase, which naturally stabilizes this phase and therefore lowers the transition temperature.

In order to better understand the spin-reorientation observed experimentally, our CEMS measurements were accompanied by theoretical calculations carried out in the framework of density-functional theory (DFT), using the local spin density approximation (LSDA). To calculate the electronic structure, the fully relativistic Korringa-Kohn-Rostoker (KKR) Green' s function band structure method in multiple scattering formulation was applied [31]. To integrate over the 3D Brillouin Zone (BZ) a regular $\boldsymbol{k}$-mesh of ~10^5 points in the whole BZ was used. For the angular momentum expansion of the Green's function a cutoff of $l_{max} = 3$ was applied.

The magneto-crystalline anisotropy (MCA) is studied by means of magnetic torque [32] calculations. The component $T_u(\theta,\varphi) = -\partial E(M(\theta,\varphi))/\partial\theta$ of the magnetic torque $\boldsymbol{T}$ acting on the magnetic moment $\boldsymbol{M}$ was calculated, which is aligned along the direction $\boldsymbol{u}$ orthogonal to $\boldsymbol{M}$ and lying in the plane perpendicular to the *z*-axis. T_u (θ,φ) is characterized by the angles θ and φ with respect to z- and x-axes, respectively. A special choice of the geometry for the torque calculations, *i.e.* $\theta = \pi/4$ and $\varphi = 0$, gives access to the energy difference E[100]-E[001]; the MCA within the film plane was not analyzed because of its small value.

To compare directly with experiment, the theoretical calculations have been performed using the experimental lattice constants of the FeRh thin films, derived from our x-ray diffraction data, and assuming perfect chemical and structural order. The spin-resolved electronic structure of FeRh has been calculated for the system in FM and AFM states with compressive and tensile tetragonal distortion. The element-resolved spin magnetic moments are presented in Table I. Note that the temperature-induced transition from the AFM to the FM state is accompanied by a ~ 0.8 % increase in c/a ratio due to the anisotropic lattice expansion for both samples, but neither crosses c/a=1. This leads to a corresponding increase of the Fe spin magnetic moment by ~ 3 % upon the AFM to FM transition, as already observed in previous calculations [1], which is in qualitative agreement with the experimental increase of the hyperfine field by ~ 6 %.

The MCA energy of the FM and AFM states is plotted in Fig. 3 as a function of the c/a ratio, exhibiting a nearly-linear dependence for each magnetic state. The tetragonal distortion breaking the cubic symmetry of the system results in a modification of the electronic structure, which leads to an energy difference between the states with out-of-plane and in-plane magnetization directions. By varying the spin-orbit coupling (SOC) of each component away from its actual value, we find a pronounced decrease of the MCA when the SOC for Rh approaches zero, both in FM and AFM states, which indicates the important role of the Rh atoms for the MCA in FeRh films. While in the FM state the hybridization is different for spin-up and spin-down states, resulting in a non-zero magnetic moment, in the AFM state the hybridization is similar for both spin directions, leading to $m_{Rh} = 0\ \mu_B$. Although the net Rh spin magnetic moment in the AFM state is equal to zero, the electronic states of Rh are strongly hybridized with those of Fe [6,16], which makes them sensitive to the direction of the magnetization. This difference in hybridization is likely to be responsible for the opposite MCA energy calculated for the two magnetic phases. Such a SOC-induced anisotropy effect has been obtained theoretically on Mn_2Au and MnIr, two other bimetallic antiferromagnets [33], but the linear dependence of the MCA as a function of strain, the possibility of generating perpendicular magnetic anisotropy, and the flexibility offered by epitaxial growth to manipulate the strain was not considered there.

Thus, in the case of c/a < 1 (corresponding to FeRh//IBAD-MgO) the calculations yield the out-of-plane (z-direction) easy magnetization direction for the AFM state (c/a=0.985) and in-plane easy direction for the FM state (c/a=0.993), in full agreement with the experiment. When c/a > 1 (corresponding to FeRh//MgO), the AFM state (c/a=1.008) has an in-plane anisotropy, as found experimentally, and the FM state (c/a=1.016) an out-of-plane MCA direction, while experimentally a broad distribution of Fe moment orientation was seen for the FM phase. Note, however, that the results presented in Fig. 3 do not account for the shape anisotropy, whose value deduced from the magnetization data (at 400 K) is $\sim 7.6\times10^5$ J/m^3 (1.28×10^{-4} eV/f.u.). Calculation of the MCA for c/a=1.016 gives 0.45×10^{-4} eV/f.u., a factor of 3 smaller than the shape anisotropy. The existence of out-of-plane moments could result from an underestimate of the MCA by the DFT calculation [34], or from a low anisotropy magnetic domain configuration in which magnetic moments point out-of-the plane, even though the MCA energy is lower than the demagnetizing energy [35]. Since the latter favors an in-plane configuration of the magnetic moments, the fact that the direction of the Fe magnetic moments was experimentally found to be distributed over a broad range of orientations in the FM phase of FeRh//MgO indicates the onset of a spin-reorientation towards the normal to the film plane, and suggests the possibility of stabilizing a perpendicular FM phase for a higher c/a ratio.

It should be noted that perpendicular anisotropy in FM FeRh (001)//MgO (001) had already been suggested in [36] based on magnetization measurements showing coercivity along the hard axis; that is however weak evidence and no theoretical calculations were performed to understand the origin of this

observation. It is important to mention that while Cao *et al.* [36] attributed this spin reorientation to magnetoelastic anisotropy originating from the lattice expansion across the magnetic phase transition (meaning it would exist only in the FM phase), our work shows that it actually results from the magnetocrystalline anisotropy and exists in both magnetic phases.

In summary, we have demonstrated that strained FeRh undergoes a spin reorientation through the AFM-FM metamagnetic phase transition, which is very well confirmed by first-principles calculations accounting for epitaxial strain. The excellent agreement between theory and experiment indicates that the spin reorientation is driven by strain, and is tuned by the use of different substrates. It is important to note that bulk samples do not exhibit such a spin reorientation since the magnetocrystalline anisotropy is zero for c/a=1 in both phases. This effect is therefore specific to thin films and is likely to be even larger in thinner films such as those contemplated for TAMR. Strained thin films could be of considerable interest for future applications based on AFM spintronics, and the possibility of getting a FM FeRh thin film with perpendicular anisotropy deserves attention.

The authors would like to acknowledge Asif Khan for the high-temperature X-ray diffraction measurements, and Randy Groves and Bruce Clemens for the growth of the IBAD MgO films. Research was supported by the U.S. Department of Energy, Office of Science, Office of Basic Energy Sciences, Division of Materials Sciences and Engineering under Contract No. DE-AC02-05CH11231 [Baldasseroni, Bordel, Cooke and Hellman], ANR Pnano through Contract No. ANR-08-NANO-035 "NAMAMIS" [Juraszek], SFB689 [Mankovsky, Minár, Ebert], and growth of the films at UCSD was supported under DOE-BES Award No. DE-SC0003678 [Moyerman, Fullerton].

REFERENCES

1. V. L. Moruzzi and P. M. Marcus, Phys. Rev. B **46**, 2864 (1992).
2. M. E.Gruner, E. Hoffmann, and P. Entel, Phys. Rev. B **67**, 064415 (2003).
3. R. Y. Gu and V. P. Antropov, Phys. Rev. B **72**, 012403 (2005).
4. C. Stamm *et al.*, Phys. Rev. B **77**, 184401 (2008).
5. J.-S. Lee *et al.*, Phys. Rev. B **82**, 224410 (2010).
6. L. M. Sandratskii and P. Mavropoulos, Phys. Rev. B **83**, 174408 (2011).
7. J.-U. Thiele, S. Maat, and E. E. Fullerton, Appl. Phys. Lett. **82**, 2859 (2003).
8. J.-U. Thiele *et al.*, IEEE T. Magn. **40**, 2537 (2004).
9. M. Fallot, Ann. Phys. **10**, 291 (1938).
10. F. de Bergevin and L. Muldawer, Compt. Rend. **252**, 1347 (1961).
11. F. de Bergevin and L. Muldawer, Bull. Am. Phys. Soc. **6**, 159 (1961).
12. J. S. Kouvel and C. C. Hartelius, J. Appl. Phys. **33**, 1343 (1962).
13. G. Shirane *et al.*, Phys. Rev. **131**, 183 (1963).
14. P. Tu *et al.*, J. Appl. Phys. **40**, 1368 (1969).
15. C. Koenig, J. Phys. F Met. Phys. **12**, 1123 (1982).
16. A. Gray *et al.*, Phys. Rev. Lett. **108**, 257208 (2012).
17. David W. Cooke *et al.*, *submitted to Phys. Rev. Lett.*, ID#LR13567.
18. J.-U. Thiele, M. Buess and C. H. Back, Appl. Phys. Lett. **85**, 2857 (2004).
19. G. Ju *et al.*, Phys. Rev. Lett. **93**, 197403 (2004).
20. I. Radu *et al.*, Phys. Rev. B **81**, 104415 (2010).
21. S. O. Mariager *et al.*, Phys. Rev. Lett. **108**, 087201 (2012).
22. V. E. Kuncser, *et al.*, Phys. Rev. B **68**, 064416 (2003).
23. W. A. A. Macedo *et al.*, Phys. Rev. B **70**, 224414 (2004).
24. F. Stromberg *et al.*, Phys. Rev. B **72**, 064440 (2005).
25. J. Juraszek *et al.*, Rev. of Sci. Instr. **80,** 043905 (2009).
26. David W. Cooke *et al.*, Rev. of Sci. Instr. **82**, 023908 (2011).
27. J. Teillet, F. Varret and J. Juraszek, MOSFIT program (unpublished).
28. B. Scholz, R. A. Brand and W. Keune, Phys. Rev. B **50**, 2537 (1994).
29. J. van Driel *et al.*, J. Appl. Phys. **85**, 1026 (1999).

30. S. Maat, J.-U. Thiele and Eric E. Fullerton, Phys. Rev. B **72**, 214432 (2005).

31. H. Ebert, D. Ködderitzsch and J. Minar, Rep. Prog. Phys. **74**, 096501 (2011).

32. J. B. Staunton *et al.*, Phys. Rev. B **74**, 144411 (2006).

33. A. B. Shick *et al.*, Phys. Rev. B **81**, 212409 (2010).

34. O. Eriksson *et al.*, Phys. Rev. B **42**, 2707 (1990).

35. D. M. Donnet, K. M. Krishnan and Y. Yajima, J. Phys. D: Appl. Phys. **28**, 1942 (1995).

36. J. Cao *et al.*, J. Appl. Phys. **103**, 07F501 (2008).

TABLES

	AFM				FM				
	a=b (Å)	c (Å)	c/a	$\mathbf{m_{Fe}}$ **(μ_B)**	a=b (Å)	c (Å)	c/a	$\mathbf{m_{Fe}}$ **(μ_B)**	$\mathbf{m_{Rh}}$ **(μ_B)**
FeRh//MgO	2.980	3.004	1.008	**3.139**	2.980	3.028	1.016	**3.228**	**1.016**
FeRh//IBAD MgO	3.005	2.959	0.985	**3.095**	3.005	2.983	0.993	**3.199**	**1.020**

Table I: Room temperature lattice constants (measured for the AFM phase and extrapolated for the FM phase using the experimental linear thermal expansion coefficient of 1.13×10^{-5} K^{-1}, as determined from the thermal variation of the out-of-plane lattice constant), corresponding c/a ratio, and calculated spin magnetic moments (bold) of FeRh thin films in the AFM and FM phases.

FIGURES

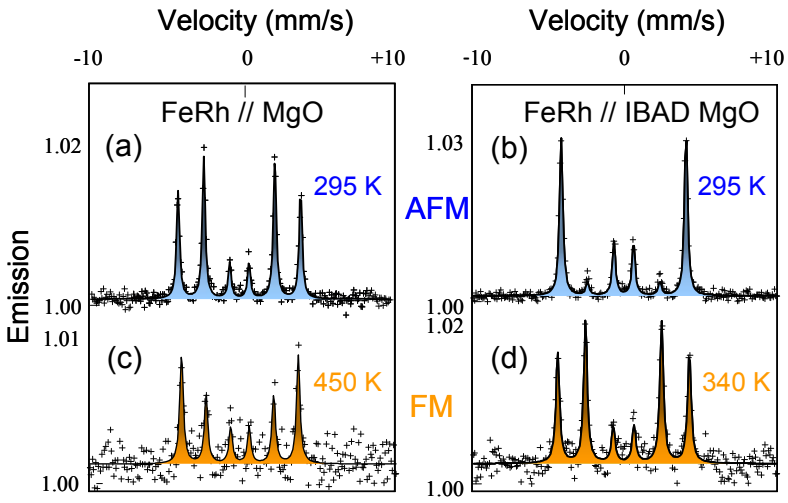

Fig. 1: CEMS spectra obtained at different temperatures on (a,c) $Fe_{0.98}Rh_{1.02}$//MgO and (b,d) $Fe_{0.98}Rh_{1.02}$//IBAD MgO. The room temperature spectra (a,b) correspond to the AFM phase and the high temperature spectra (c,d) to the FM phase. Note that (c) was obtained upon heating and (d) upon cooling.

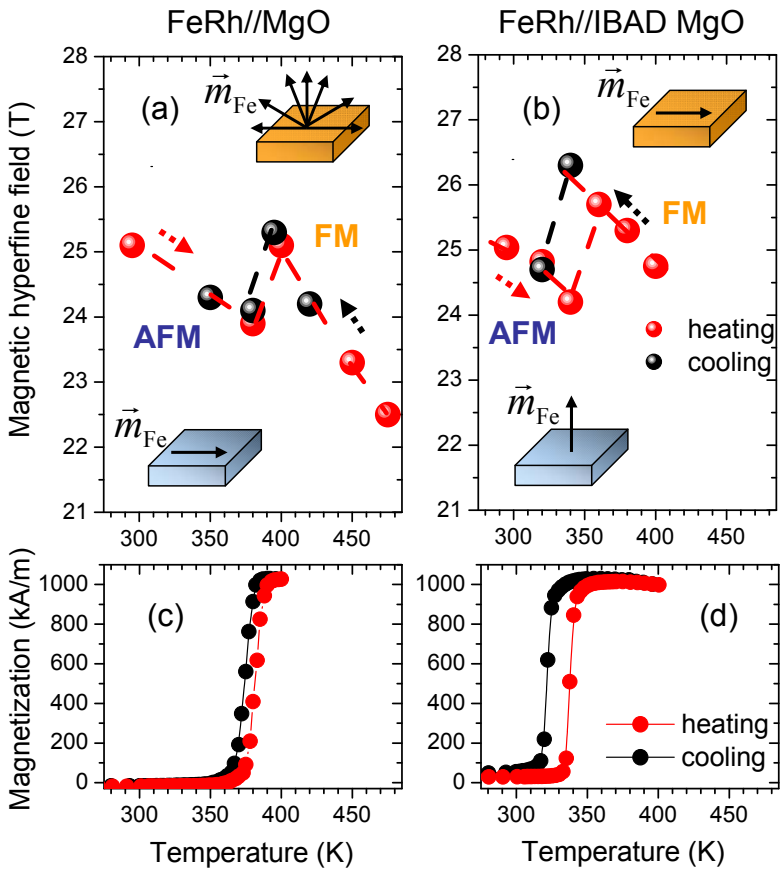

Fig. 2: Temperature dependence of the hyperfine field upon heating and cooling for (a) $Fe_{0.98}Rh_{1.02}$//MgO and (b) $Fe_{0.98}Rh_{1.02}$//IBAD MgO. Insets show the Fe moment orientation with respect to the sample plane in both AFM and FM phases for each sample. Temperature dependence of the magnetization (measured under 1 T and extrapolated in zero field using the experimental coefficient of 8 K/T) upon heating and cooling for (c) $Fe_{0.98}Rh_{1.02}$//MgO and (d) $Fe_{0.98}Rh_{1.02}$//IBAD MgO.

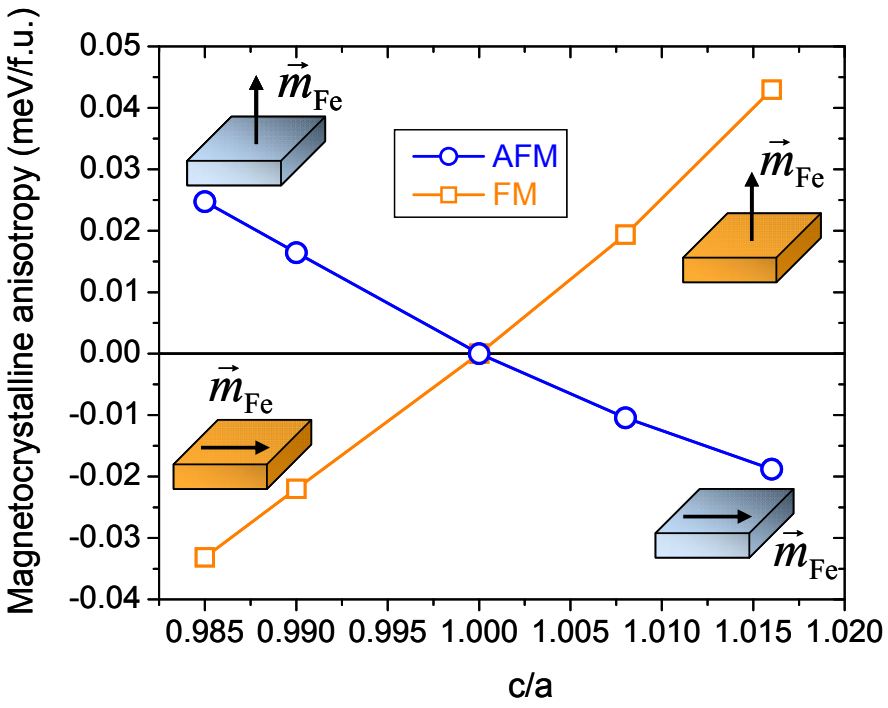

Fig. 3: MCA energy calculated as a function of the c/a ratio for each of the two magnetic phases.